To be published in Physics Today,
Vol. 31, No. 10

LBL-8367
Preprint

THE TIME PROJECTION CHAMBER

D. R. Nygren and J. N. Marx

July 1978

Prepared for the U. S. Department of Energy
under Contract W-7405-ENG-48

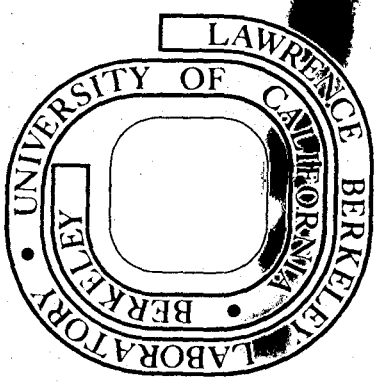

DISCLAIMER

THE TIME PROJECTION CHAMBER

D. R. Nygren and J. N. Marx

Lawrence Berkeley Laboratory
University of California
Berkeley, California 94720

July 1978

Introduction

Progress in experimental high energy physics is limited in practice by two complementary aspects: 1) the types of beam particles available with useful intensities and energies, and 2) the characteristics of the detection techniques available for measuring needed information about collisions of interest and their subsequent reaction products. Most impressively, advances in accelerator design over the last three decades have led to an increase in beam energies of nearly three orders of magnitude, and the advent of colliding beam machines has brought a comparable increase to the center-of-mass energy available. The diversity of useful beam species has now grown to include essentially all known particles with lifetimes greater than 10^{-11} seconds.

On the other hand, the number of well-developed important fundamental techniques for particle detection and measurement has remained limited. In addition to continuously sensitive devices such as photographic emulsions, Cerenkov, scintillation, ionization and drift-proportional wire detectors, triggered devices such as bubble, spark and streamer chambers essentially exhaust the list of commonly used techniques.

The challenge posed by this contrasting state of development is particularly evident in the design of experiments for the newest generation of electron-positron colliding beam machines such as PEP and PETRA.[1] Here, a single interesting collision may produce on the order of twenty charged and neutral particles, with a wide variety of interesting (and possibly new!) quantum numbers. To compound the difficulty, the distribution of particle trajectories is expected to be nearly isotropic when averaged over many events, but within a given event the trajectories may cluster together in a pronounced "jet" structure. This situation translates into an unusually demanding and conflicting set of requirements for detector performance, for which a completely satisfactory solution utilizing conventional techniques does not appear to exist. The resultant frustration was the seedbed leading to the conception of the Time Projection Chamber (TPC) idea.

The motivation to find a new solution for the problem of particle detection and identification at PEP energies is particularly strong. At SPEAR and DORIS, the lower energy predecessors of PEP and PETRA, an important new window to the subnuclear world has been opened for experimental investigation. Major discoveries such as the hitherto unknown family of hadrons with a new quantum number, "charm", and a heavy lepton, called τ, have already been made at these energies.[2] The

PEP and PETRA storage rings will extend the center-of-mass energy in electron-positron collisions to above 30 GeV, more than a four-fold increase over that available in SPEAR. This new energy regime is expected to provide discoveries of at least comparable significance.

PEP and PEP Physics

The main component of PEP is a single ring of magnets enclosing a high vacuum chamber through which counter-rotating beams of electrons and positrons circulate. Each beam is concentrated into three very short bunches so that beam-beam collisions occur only at six equally spaced "intersection regions" placed around the ring. The magnet ring itself is divided into six bending arcs connected by long straight sections passing through the intersection regions. This gives the ring a rounded hexagonal shape with an overall circumference of 2160 meters. Consequently, beam bunches pass through each other every 2.4 microseconds.

The event rates of interest, however, are quite small. The fundamental physics interest will presumably arise in electron-positron annihilation reactions, mediated by a single massive virtual photon intermediate state (see Figure 1a). Here the entire center-of-mass energy is converted to a large variety of final states, limited only by conservation laws governing interactions with photons as the intermediate state. To give some idea of rates, the number of $e^+ + e^- \to \gamma^* \to \mu^+ + \mu^-$ events per hour, at peak luminosity, is only 30. This example points out one property of paramount importance required of any PEP or PETRA detector: sensitivity over most of 4π steradians. Every effort must be made to detect and measure completely all events of interest.

The study of muon pair production at PEP energies is of considerable interest not only a precise test of Quantum Electrodynamics but also as a reaction which may display measurable effects arising from interference of the one photon annihilation amplitude with a neutral weak current amplitude due to the existence of the proposed weak neutral boson, Z^0 (see Fig. 1b). These observable effects could include violations of parity and charge conjugation invariance evidenced by forward-backward asymmetry in the angular distribution with respect to the beam direction. In order to confront themodel dependence of the weak-electromagnetic unification theories, a statistical precision of 2% is needed.[3]

The production of hadrons at PEP energies is also expected to provide data of major interest. In the one photon annihilation process, hadrons are thought to be produced through pair production of a quark-antiquark state. In this poorly understood model the quark and antiquark then each materialize as a jet of hadrons which carry off the momentum and quantum numbers of the initial quarks. Figure 1c illustrates these processes. In this model the hadron production cross section is related to the muon pair production cross section in a particularly simple manner. Specifically, the assumption that quarks respond to the electromagnetic interaction as pointlike fermions differing only from muons in charge and mass leads to the following result at high energies. Let R be the ratio of the total cross section for hadron production to the total cross section for muon pair production. Then R is equal to the sum of the squares of the electric charges of all quark species able to contribute. As the electron-positron energy increases,

new thresholds may be exceeded allowing new species of quarks to contribute, leading to a noticeable change in R. The measurement of R alone thus provides an uncommonly useful insight into the fundamental constituents of matter.[4] The careful measurement of R at PEP energies will be of high priority, but will also place severe demands on the capability of the detector to react to and measure hadronic final states of great diversity. Extrapolating SPEAR data to PEP energies, R is expected to fall between 5 and 10. The number of hadronic events per hour may therefore be in the range of 150 to 300.

The extrapolation of the lower energy data also suggests that on the average about 15 particles per event will be produced, about half of these will be neutral, and that the "jet" characteristic will be a pronounced feature of the events. The axes of the jets are expected to be distributed nearly isotropically in space. The identification of particle species within the jets is of singular importance in order to untangle the primary production processes from the decays of very short-lived states leading to the observed long-lived particles.

The tasks of detection and detailed measurement of these hadronic jet events pose the most serious challenge for the design of experiments at PEP. The ideal detector system would be able to observe events over nearly 4π steradians with very high efficiency, be able to measure accurately the momentum of at least a dozen charged particles clustered closely in space, identify the species of each of the particles that make up the jets, measure accurately the energies and directions of all photons emitted, and be insensitive to uninteresting backgrounds which may be many orders of magnitude more copious.

Problems of the Conventional Approach

In the attempt to find a conventional solution to the experimental problems indicated above, several factors combine to prevent an attractive solution:

1. A conventional solenoid magnetic spectrometer with a field of about 0.5 Tesla would need a tracking length of about 1.5 meters for good momentum resolution. A system of spark or drift chambers would serve to measure tracks but provides no particle identification.

2. If complete charged particle identification is sought over the momentum span of interest at PEP by Cerenkov and/or time-of-flight methods, then a physically enormous detector is inevitable. This is because several layers of Cerenkov detectors and very long flight paths would be required. The additional radius needed for these purposes would be about 3 meters. As the particles must pass through the magnet coil, interactions there compromise the quality of particle identification by detectors beyond it.

3. In order to be efficient the photon detection system must rely on total absorption through shower development in a high Z material like lead. Due to the strong scattering and attenuation of charged particles passing through the lead, the photon detection system must necessarily lie beyond the charged particle identification system. Thus the photon detection system would be required to cover huge surface areas with many multi-ton multi-layer shower sampling devices.

4. The important task of distinquishing muons from pions and other hadrons must be carried out beyond even the photon detection system as muons are best identified by their unique penetrating power. In practice their detection is usually carried out by absorbing all other charged particles in about one meter of steel,and labeling any emergent trajectory as a muon.

Thus the outer layer of this detector approach would be a shell of steel about 10 meters in diameter, covered with track sensitive detectors. Total weight of the detector would be about 3000 tons, dominated by the muon detector.

5. To deal with the expected jet structure of the event, the tracking, charged particle identification, photon, and muon systems would be required to have a high degree of solid angle segmentation so that track pile-up and resultant ambiguities might be minimized. Monte Carlo studies indicate that several hundred individual Cerenkov cells would be needed. Furthermore, low momentum tracks which are confined within the tracking system by the solenoid magnetic field cause serious problems in pattern recognition.

This fictitious detector scheme is too ponderous and expensive to survive the competitive rigors of the approval process, but it does serve to illustrate why an ambitious new approach may be welcomed if it carries the promise of the needed performance at an acceptable cost.

Time Projection Chamber: Conception and Evolution

The above discussion suggests that a substantial advance would be realized if the particle identification function could be combined within the same detector volume as the tracking and momentum measurement functions. As the latter inevitably depend on the processes by which charged particles lose energy in matter, it is of considerable interest to examine this phenomenon to see whether useful information for particle identification may be obtained. Specifically,we wish to examine the energy loss in a very thin sample of gas, e.g. one cm at STP, as this corresponds to a typical sensitive region of a drift or proportional wire chamber.

The most probable energy loss in an argon-methane mixture is shown as a function of momentum for a variety of interesting particles in Figure 2. The family of curves actually represent a single expression which depends only on the sample thickness and composition on the particle charge and velocity.[5] Except for the troublesome points where the curves cross, measurement of the ionization density does appear to offer a potentially useful means of distinquishing between particles with the same momentum but different velocity. It is clear from Figure 2 that high resolution measurements of momentum and ionization density are needed to minimize the regions of ambiguity found at the crossing points of the curves.

The expression represented in Figure 2 is a modern version of the Bethe-Bloch Formula and for our purposes may be divided into three regions of interest: 1) the nonrelativistic regime, $\beta\gamma \lesssim 2$, where the dominant dependence of the expression is as the inverse square of β. The sensitivity here is obviously strong, and makes particle identification relatively easy. 2) a relativistic regime, $2 \lesssim \beta\gamma \lesssim 100$ where the ionization density instead of falling passes through a minimum and then increases logarithmically with $\beta\gamma$ as a consequence of the relativistic compression of the electric field of the particle. Particles of considerable interest such as kaons and protons are expected to be produced frequently at PEP in this $\beta\gamma$ range, arguing for measurements of the ionization density with at least 3% rms resolution. 3) An ultra-relativistic regime, $100 \ll \beta\gamma$, characterized by a gradual levelling due to increased effects of polarization of the medium by the relativistically compressed electric field. At PEP only electrons are expected to be found in this regime. The $\beta\gamma$ value for the onset of

leveling out to the "Fermi Plateau" depends on the density as well as the polarizability of the medium, so that only gases show an appreciable rise from the minimum around $\beta\gamma = 3.3$.

How well can one measure the most probable energy loss, or better, what is the optimum way to extract information about velocity from the observed energy loss? The distribution of energy losses for particles passing through 6 mg/cm^2 of argon-methane is shown in Figure 3, as measured by a prototype time-projection chamber. The characteristic asymmetry, skewed towards high energy losses, is a feature well-known to experimental high energy physicists, even those used to working with much thicker absorbers such as plastic scintillator. This "Landau tail" is a result of the very broad $1/E^2$ spectrum of knock-on electrons produced by occasional close encounters with the atomic electrons. The nature of this spectrum precludes the applicability of the central-limit theorem so that the resolution obtainable with a thick absorber is not much better than that obtainable with a very much thinner one. Conversely, the resolution obtainable with many thin absorbers can be much better than that obtained from a single absorber of equal total thickness, providing that the occasional large energy loss fluctuations are eliminated from the data. For example, suppose a particle passes through 200 individual proportional chambers and the resultant pulse height ensemble is ordered according to amplitude. The average of, say the lowest 100 pulse heights is taken, and the values compared after further repititions are made with identical particles. The resolution obtained by this truncated mean method is significantly better, perhaps by a factor of three, than if the average of the entire ensemble of samples is taken. Furthermore, the resolution is relatively insensitive to the

fraction of samples retained over the range 30% to 70%. The prescription for the detector design is clear: provide enough gas and sample the ionization enough times so that at least 3% rms resolution is obtained.

The detailed study of this question shows that a track length of about 4 to 8 meters through a typical gas at STP is needed, and that there should be at least 100 samples taken. This would at first appear to cast a rather dark cloud over the whole approach, but unlike the Cerenkov or time-of-flight technique, gas is easily compressed. Beyond the direct mechanical problem of containment, though, compressing the gas by a factor of 10 to achieve a more reasonable detector size also has the undesirable consequence that the ionization density reaches its asymptotic value at a lower value of $\beta\gamma$, thereby reducing the total rise from that shown in Figure 2. Nevertheless, the technique appears sufficiently encouraging that we now consider the question of what sort of detector geometry should be employed to obtain the sampling needed. This question however, must be considered in parallel with the problem described earlier, of how to obtain spatial information of sufficiently high quality to reconstruct all the trajectories, even within jets.

A number of variations of the conventional approach were considered and found unattractive. These would usually involve a huge number of drift proportional wires parallel to the magnetic field in order to measure the particle's curvature accurately and to obtain the necessary number of samples for ionization information. No convenient method was found to obtain good spatial information for the longitudinal coordinate, i.e.

where the track crossed along the wire. Furthermore, since the drift electrical field was perpendicular to the magnetic field, $\vec{E} \times \vec{B}$ forces substantially alter the electron drift velocity and drift direction through the gas, complicating the relationship between drift time and trajectory position.

"Well, what would happen if the drift electric field direction is rotated to become parallel to the magnetic field?" This simple question posed by one of us (DRN) when the end of the conventional road seemed unescapable, immediately led to a number of new possibilities culminating in the formulation of the time-projection chamber concept.[8]

If the magnetic and electric drift fields are exactly parallel, then the absence of $\vec{E} \times \vec{B}$ forces invites the consideration of very long drift distances for the ionization electrons, such as a meter or more. A practical limit, however, will be set by the total amount of voltage needed to generate the drift field over long distances. An examination of likely gas mixtures showed that argon-methane display exceptionally high electron mobilities, leading to the lowest total voltage requirement for a given drift velocity. Electron capture by electronegative molecules over a long drift interval is another possible limitation, but oxygen and water, the most common problem are easily removed from argon and methane by commercial purifiers.

An ultimate upper limit to the drift distance will be set by the degradation of track information due to diffusion of the ionization electrons as they drift through the gas. The diffusion grows only as the square root of the drift length, and was soon recognized to be reduced substantially by the presence of a magnetic field.[9] The spatial distribution of an ideal point swarm of electrons after a time T is described by a Gaussian form

of width $\sigma = \sqrt{2DT}$, where σ is the rms normal distance to a plane containing the origin of the swarm. In the presence of an electric drift field this expression may be rewritten approximately as $\sigma = \sqrt{2DL/W}$ where L is the drift length and W is the aggregate electron drift velocity. The diffusion coefficient D is given by $D \equiv V\ell/3$ where V is the electron speed (related directly to the temperature of the electrons) and ℓ is the electron mean free path in the gas under consideration. In the presence of a parallel magnetic field, D is modified by a factor $(1 + \omega^2\tau^2)^{-1}$. Here ω is the electron cyclotron frequency eB/mc and τ is the electron mean time between collisions. The diffusion parallel to the field is unaffected by the presence of a magnetic field, but the spatial resolution requirements in this direction are quite modest.

An experimental study[10] was made of several mixtures of argon-methane to measure quantitatively the diffusion transverse to the drift field direction with and without the presence of a parallel magnetic field. The results, taken near atmospheric pressure, are shown in Figure 4. The surprisingly large suppression of transverse diffusion at atmospheric pressure, corresponding to large values of the dimensionless parameter $\omega\tau$, is a providential consequence of the Ramsauer-Townsend effect in argon. This purely quantum-mechanical phenomenon leads to a very deep minimum in the electron-argon cross-section at energies of about 1/3 eV. In effect, the argon and to a less extent the methane, after contributing ionization, conveniently "disappear" during the drift of the ionization electrons, allowing quite a small drift fields to be employed.

The data of Figure 4 can be scaled to various values of the magnetic field, pressure, and drift length using the relationships given above.

For example, the rms transverse diffusion for 1.5 Tesla, 10 atmospheres, and one meter is typically slightly more than one mm for practical values of the drift field. To be competitive with drift chambers a transverse spatial resolution of 0.2 mm is needed, forcing a closer look at the information content of the track.

At 10 atmospheres, about 400 ionization electrons are liberated per cm of track length in argon-methane. Each electron carries information, and if a readout technique is found which weights each electron equally, then a substantial improvement is possible. The improvement factor in this example, if each electron were weighted equally and the electron origin were an ideal point source, would be $(400)^{-\frac{1}{2}}$ due to the Gaussian nature of diffusion. In practice the proportional amplification around a wire fluctuates due to statistical effects and the electron source is a highly variable particle trajectory. Nevertheless, a detailed study shows that a spatial resolution better than 200 microns should be possible if a technique is used that is sensitive to all of the ionization electrons.

The practical solution here was already at hand. Dr. G. Charpak and his colleagues at CERN had demonstrated that the positive signals induced on all electrodes near a proportional avalanche preserve most of the information of the track. These signals, due to the motion of the positive ions generated by the avalanche process near a proportional wire, can be sensed easily by low-noise amplifiers connected to a segmented cathode. The center-of-gravity of the induced signals provides a very high resolution estimate of where a track element falls along a proportional wire (see article by Charpak, this issue).

The concept of the Time-Projection Chamber in the PEP environment was now nearly complete. A cylindrical volume of pressurized argon-methane would surround the beam-beam crossing point. A central conducting membrane would be connected to a large negative voltage, as much as 150 kilovolts, electrostatically dividing the cylinder into 2 symmetric halves. Accurately constructed voltage dividing cages around the beam pipe and outer wall would complete the drift field generating structure. Since momentum resolution and the TPC both benefit from strong magnetic fields, a superconducting solenoid would be employed to superimpose a field of 1.5T parallel to the drift electric field (see Figure 5).

The ionization electrons generated by the passage of charged particles through the gas would be translated by the drift fields toward each end of the cylinder where a single layer of proportional wire readout planes would amplify and detect the arriving electrons. The primary tasks of the two readout planes are to sample the ionization density of all track images and to provide high quality spatial information such that the trajectories associated with the ionization can be efficiently and accurately reconstructed.

It was immediately clear that if the cathode surfaces of the readout planes were sufficiently well-segmented, then the spatial data would possess a unique three-dimensional quality, of enormous benefit to pattern recognition and reconstruction of complex events. In other words, it seemed possible to construct the cathode so that a pair of othogonal coordinates could be obtained for a track segment in a very localized way; the third orthogonal coordinate would be obtained by measuring the drift time of the track segment relative to the beam crossing time. Figure 6 shows a simplified view of a TPC readout plane with just two wires depicted for clarity.

Track segments drift onto and are amplified by avalanches near the proportional sense wires; the cathode just behind the sense wire is locally segmented into a strip of "pads" of 0.8 cm x 0.8 cm size. The 2 or 3 pads nearest the avalanche experience induced signals which vary rapidly in amplitude with distance from the site of the avalanche. As all incident electrons contribute to these induced signals, the center of gravity of the pad's response accurately provides the avalanche coordinate along the wire, and in a way that is unaffected by the presence of other simultaneous avalanches due to tracks a few cm away. The pads and wires must be equipped electronically to provide high resolution analogue information as well as the drift times associated with the analogue signals. A typical track image can be sensed by many proportional wires with locally segmented cathodes. The resultant set of three dimensional data points define the trajectory with high accuracy and little interference from nearby tracks.

For comparison, the usual practice of employing crossed wire planes to measure projections of a particle trajectory will, for N tracks, produce N^2 possible combinations of coordinate pairs. The correct pairings can only be determined by use of additional planes at other angles, but the problem has proven to be unpleasantly difficult for high track multiplicities in the presence of strong magnetic fields. In the TPC, spatial projections are essentially absent, and the only projection is in time, along the drift direction.

An overall view of the actual TPC readout planes are shown in Figure 7. Each surface is divided into six identical and electrically independent wedge-shaped sectors. Each sector contains a set of 192 proportional

wires parallel to each other and perpendicular to a radial line through the center of the wedge. The space between the wires is 4 mm. All 192 wires act to provide samples of the ionization density of tracks which drift onto them. Independent of the trajectory dip angle, any track image (trail of ionization electrons) within the sensitive volume eventually drifts completely onto this array. The cathode plane behind twelve of these wires, in equally spaced radial intervals is locally segmented into pad rows to provide the track coordinates along the direction of these special wires.

The actual configuration of the readout plane includes a grid 4 mm in front of the sense plane and an additional array of 193 thicker "field" wires in the sense plane and spaced half-way between the sense wires. The grid serves to separate the drift region from the amplification region permitting independent control of these functions, and to capture positive ions generated by the avalanche process near the sense wire. The field wires serve to improve the electrostatic stability of the wires and to reduce the cross talk of induced signals from neighboring sense wires on each other. The electrostatics of the actual configuration are depicted in Figure 8. Because the amplification region has a much stronger electric field than the drift region, an extremely small fraction of the incident electrons wind up on the grid, as shown by the dashed lines in this figure.

The positive ions generated by the avalanche process, although crucial for the detection of signals in the readout plane, turn out to introduce a particularly nasty space charge effect as they enter and pass back through the drift region, migrating slowly to the central high voltage membrane. Although the boundary surfaces of the TPC are well-defined in potential, the positive ion space charge can modify the electric field

substantially within the drift volume. Any radial electric field component directly, and indirectly though the $\vec{E} \times \vec{B}$ force, distorts the track images as they drift. At PEP, the dominant source of ionization electrons in the TPC are due to machine-induced backgrounds such as synchrotron radiation. Calculations show that a narrow margin of safety should exist if the proportional wire gain is kept as low as possible. The positive ion space charge problem at present is an important limitation on the applicability of the TPC technique to other areas of potential use.

The electronic complement needed to process the wire and pad signals begins with a low-noise charge-sensitive preamplifier located within a few cm of the signal source. Next, a remote amplifier shapes the signal to optimize resolving time and pulse height resolution. The shaped response signal for each wire or pad is then introduced into an analogue storage device, which is capable of storing both pulse height and time information. The storage devices are really analogue shift registers, a recent development in semiconductor technology known as charge-coupled devices (CCD's). The CCD's sample the input waveform at a rate determined by an external clock. The resultant levels are shifted along until the entire history of an event is completely stored, a time interval corresponding to the maximum drift time. As a typical electron drift velocity is six to seven cm/microsecond, this interval for a one meter drift length is about 16 microseconds. Commercially available CCD's operate in the range of 15 MHz so that approximately 240 samples may be taken, corresponding to a sampling interval in the drift direction of 4 mm. In the absence of an event trigger, the CCD clock runs continuously, spilling the uninteresting information appearing at the CCD output. The appearance of an event

trigger causes the CCD clock to slow down after the assimilation period is finished to a rate comfortable for conventional analogue-to-digital circuitry. The slow clock rate may be as low as 20-50 KHz, corresponding to a time expansion factor of several hundred. The CCD's essentially permit the TPC to be subdivided electronically into several million relatively independent sensitive volumes, an impossibility by physical means.

TPC DEVELOPMENT PROGRAM

Many of the operating principles of the TPC are being tested with a prototype which is now operating at the Lawrence Berkeley Laboratory Bevalac in a charged particle beam line equipped with time-of-flight and Cerenkov detectors. To fit the geometry of locally available dipole magnets, the sensitive area of the prototype is rectangular instead of wedge shaped, and the maximum drift distance is just 10 cm (see Figure 9) In most other respects it resembles closely the TPC designed for PEP. The readout plane is constructed with electrostatics as shown in Figure 8 with 192 active sense wires, eight of which are operating with segmented cathode for spatial and momentum measurements.

Results obtained thus far are quite encouraging. The truncated mean energy loss for pions at 1.8 GeV/c has been measured, displaying an rms resolution of 2.7%, obtained by keeping the lowest 70% of the wire signals in the average . At this momentum, protons and pions have nearly the same most probable energy loss (see Figure 2) but due to the difference in velocity a slightly different shape in the observed energy loss spectrum exists. By using a more sophisticated statistical algorithm based on likelihood concepts, the data allow us to choose the correct

identity 75% of the time.

The spatial resolution has been studied in the prototype by fitting tracks to a curve. Using an approximate form of the pad response function, the residuals to the fit have been found to be distributed with an rms value of 140 microns. A better understanding of the pad response and improved calibration may lower this value to near 100 microns. The work done thus far with the prototype and related electronics, including data taken with CCD's in the signal processing chain, convince us that the TPC will perform at PEP as expected.

PEP FACILITY

The TPC is the core of a complex configuration of detectors being developed for PEP by a collaboration of about 50 physicists and an equal number of engineers and technicians from the Lawrence Berkeley Laboratory, University of California at Los Angeles, University of California at Riverside, The Johns Hopkins University and Yale University. The facility is expected to begin data taking operation in mid-1980. The total cost of all systems is not expected to exceed 14 million dollars. Figure 10 schematically depicts the facility, which consists of five major sub-systems.

1. The time projection chamber, which surrounds the PEP beam pipe for a length of ±1 meter and extends radially to one meter. The TPC provides pattern recognition, momentum measurement, and particle identification over more than 80% of 4π steradians. The relatively modest size of the TPC reduces the size and cost of other components at larger radii.

2. The superconducting solenoid magnet system, which provides an exceptionally uniform field of 1.5 Tesla within the sensitive volume of

the TPC. Calculated non-uniformities introduce an rms transverse distortion of the track of less than 90 microns. The coil itself is approximately 2.2 meters in diameter and 3.8 meters in length and has been designed to present a minimum of material to photons passing through it (less than 0.3 radiation length for the coil itself).

3. Cylindrical drift chambers are located at the inner and outer radius of the TPC. These chambers will be used as a part of the trigger generation and as a supplement to the TPC for the highest momentum tracks.

4. Electromagnetic shower detectors for the measurement of photon energies and directions will be constructed with thin lead plates as the shower development medium. Argon-methane gas between the plates samples the ionization, which is then amplified by proportional wires. The magnet poletips and the entire cylindrical outer surface of the magnet coil system will be equipped with shower detectors. The cylindrical shower detectors will be constructed as six planar modules to form a hexagonal shaped array. The spatial resolution of these devices is expected to be ± 2mm. The energy resolution is anticipated to be approximately 15% rms for photons of 1 GeV.

5. The remaining subsystem is a muon identifier, which employs the traditional method of absorbing all other charged particles in a thick absorber. The muon identifier for the TPC facility is a set of steel plates with 3 layers of proportional wire chambers embedded within and on the outside surface. The proportional chambers are made from aluminum extrusions with a triangular cross section to provide both strength and good detection efficiency. Muons above 1 GeV/c are detected with good efficiency by this

system. Interestingly, although ionization measurements will not be adequate to separate pions and muons in the relativistic range, nonrelativistic muons should be easily identified by the TPC.

In addition to the systems described above, a separate collaboration of physicists from the University of California campuses of San Diego, Santa Barbara, and Davis share the same interaction region with the TPC facility, and are constructing two small-angle spectrometers, also shown in Figure 10. Their apparatus is aimed at the study of non-annihilation electron-positron collisions, which are expected to display low transverse momentum characteristics. By working together, sharing data for events with particles that traverse both facilities, the sensitive solid angle for particle detection and measurement is very close to 100% of 4π steradians.

CONCLUSION

In this article we have discussed not only the principles of the TPC, but have also attempted to present some aspects of how the concept evolved. In fact, the evolution of the TPC ideas followed a somewhat more tortuous path than could be presented in this article, and has also benefited from suggestions and contributions made by many people.

New developments may lead to additional applications of the TPC such as the study of heavy-ion collisions or in proton-antiproton colliding beam experiments. Due to the very high background levels of ionizing particles expected for the proton-antiproton situation, the TPC would be feasible only if the technique could be made less vulnerable to the distortions of the drift electric field caused by positive ion feedback. An improvement here of several orders of magnitude seems possible if the grid could be transformed into an electron gate, allowing ionization

electrons to enter only when an interesting event has occurred. Since the positive ions move slowly, even the positive ions generated by the interesting event would be prevented from returning to the drift region by closing the gate soon after the electrons have entered the amplification region. If this could be achieved, the net positive ion feedback would be reduced to essentially zero.

To convert the grid into a gate may be accomplished in perhaps several ways, but one particular approach is beginning to be studied at LBL. This approach would modify the grid in two ways: 1) decrease the grid wire-to-wire spacing from 2 mm (see Fig. 8), to 1-1/3 mm, so that the cell electrostatics is as given in Figure 11a; 2) arrange alternate wires to be set at equal but opposite voltages. If the magnitude of the voltage is sufficiently high, field lines will cross from each wire to its neighbors, effectively closing the gate (Fig. 11b). When an interesting event has been detected by the trigger circuitry, the voltage differences must be rapidly and symmetrically brought to zero, to allow the drifting ionization electrons from the tracks of interest to enter. Even a tiny lack of symmetry or balance as the voltages are brought to zero will induce relatively huge signals in the sensitive wire and pad electronic circuitry, as several hundred volts are needed to close the gate. Nevertheless, the possible advantages seem attractive enough to pursue this approach.

Other beneficial developments may arise in the area of high speed analogue and digital signal processing electronics. Here, in particular, it may be risky to speculate on the future, but as the reader may have concluded by now, we are not afraid to make projections in time.

References

1) PEP, being built at SLAC by Stanford and the Lawrence Berkeley Laboratory, stands for Positron-Electron Project. PETRA, nearing completion at Hamburg, Germany, stands for Positron-Electron Tandem Ring Accelerator.

2) The discoveries of "charmed" particles and of the heavy lepton ($_{\tau}$) are described in many excellent reviews. See, for example W. Chinowsky, Ann. Rev. Nucl. Sci, 27, 393 (1977), M. L. Perl, Proceedings of 1977 International Symposium on Lepton and Photon Interactions at High Energies., DESY, Hamburg, Germany.

3) Detailed discussion of the experimental capabilities needed to confront the predictions of the various models which attempt to unify weak and electromagnetic interactions are given in the 1975 PEP Summer Study, LBL-4800, 1975.

4) S. D. Drell, Physics Today, June 1978, p. 23.

5) H. D. Bethe, Ann. Physik 5, 325 (1930), F. Block, Z. Physik 81, 363 (1933), L. D. Landau, J. Phys. USSR, 8, 201 (1944), R. Sternheimer and R. F. Peierls, Phys. Rev. B. 11, 3681 (1971).

6) A. I. Alikhanov, V. A. Lubimov, G. P. Eliseiev, Proceeding of CERN Symposium on Particle Accelerators and Pion Physics, 1956, pp 87-98.

7) The relativistic rise of the most probable energy loss is approximately 41% in the Time Projection Chamber with 4 mm samples of 80% Argon & 20% CH_4 at 10 atmospheres.

8) D. R. Nygren, "Proposal to Investigate the Feasibility of a Novel Concept in Particle Detection", LBL internal report, Feb. 1974.

9) Townsend, J, "Electrons in Gases", Hutchinson's Scientific and Technical Publications, 1947.

10) Proposal for a PEP Facility based on the Time Projection Chamber, PEP Proposal #4, Johns Hopkins University, Lawrence Berkeley Laboratory, University of California at Los Angeles, University of California at Riverside, Yale University, 1976. This document contains detailed discussions of many of the ideas discussed in this article. Diffusion on the presence of magnetic fields is discussed in Appendix A6.

FIGURE CAPTIONS

Fig. 1 Diagram of physical processes of interest at PEP.

a) The one photon intermediate state in electron-positron annihilation leading to either a multiparticle final state or to a final state containing a pair of point particles (leptons, for example).

b) The weak neutral boson intermediate state resulting from electron-positron annihilation by the "Neutral Current" Weak interaction.

c) The production of hadron jets in electron-positron annihilation through the production of a quark-antiquark intermediate state.

Fig. 2 Most probable energy loss for various species of particles in 1 cm of 80% Argon + 20% Methane at STP. Note the suppressed zero. The energy loss at the minimum corresponds to 6 KeV.

Fig. 3 Probability distribution of the energy loss of 800 MeV/c pions in 4 mm of 80% Argon + 20% Methane at 10 atmospheres. The "Landau tail" of this distribution extends to the 32.7 MeV/c, the kinematic limit for producing knock-on electrons. The distribution was obtained with a TPC prototype.

Fig. 4 a) Measurements of transverse diffusion of electrons in various argon gas mixtures as a function of E/P (volts/cm/Torr) with zero magnetic field. Drift distance is 15 cm, pressure is 600 Torr.

b) Comparison set of transverse diffusion measurements, with 20.4kG magnetic field.

c) Values of τ, the mean collision time of electrons in gas in picoseconds, and the dimensionless parameter, $\omega\tau$, as extracted from the data of figures 4a. and 4b.

Fig. 5 Schematic of the Time Projection Chamber. Magnetic and drift electric fields are parallel to the cylinder axis. Details of end caps with 192 ionization wires per sector and 12 spatial wires (with segmented cathodes) per sector are depicted in Fig. 7.

Fig. 6 Simple isometric representation of TPC readout plane depicting 8 mm x 8 mm cathode segments under proportional sense wires. The center of gravity of the signals induced on the cathode segments is used to determine the positions of the proportional avalanche along the wire. Electrons drift in the direction opposite that of the electric field.

Fig. 7 Geometry of TPC endcap wire array. 192 wires for ionization sampling (called dE/dx wires) are shown for each of six wedges. Twelve of these wires have their cathodes locally segmented into 8 mm x 8 mm pads for positional readout of the coordinate along the wire direction.

Fig. 8 Electric field configuration in the region of the Time Projection Chamber endcap wedges. Sense wire voltage = 3750 V.; field wire voltage = 400 V; grid and cathode grounded. The dashed lines depict the paths taken by electrons.

Fig. 9 Schematic view of Time Projection Chamber prototype. Drift electric field and magnetic field are normal to the plane of the drawing. Shown are 192 wires to sample ionization, eight of which have locally segmented cathodes for spacial readout.

Fig. 10 Schematic view of the PEP facility (PEP-4) incorporating the Time Projection Chamber. The beam-beam intersection point is at the center of the drawing. Shown are the Time Projection Chamber (TPC),

the drift chambers , magnet coil, calorimeters (pole tip and cylindrical),iron hadron absorbers (muon iron), and muon chambers. The Time Projection Chamber magnet coil and drift chambers are cylindrical when viewed end on; the cylindrical calorimeter, magnet yoke, hadron absorber and muon chambers form a surronding hexagonal configuration. Also shown is the 2-γ (PEP-9) detectors, a pair of spectrometers with particle identification located at small angles with respect to the beams. The 2-γ detector is being constructed by a collaboration from University of California at Davis, University of california at Santa Barbara and University of California at San Diego to study the interactions of pairs of virtual photons emitted from the beams at PEP.

Fig. 11 (a) Modified grid configuration with 1 mm wire-to-wire spacing rather than 2 mm as shown in Figure 8. With no voltage difference, electrons enter the amplification region with close to 100% efficiency.

(b) Same as a) except an alternating voltage of 250 volts has been imposed on the grid wires. The gate is closed for both electrons and positive ions.

SOME PHYSICAL AMPLITUDES OF INTEREST AT PEP

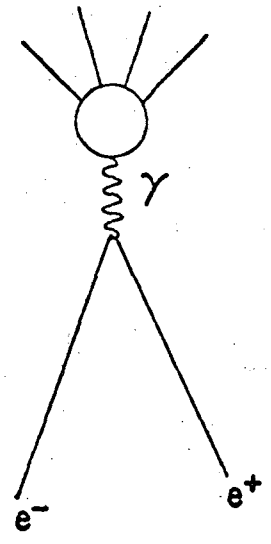

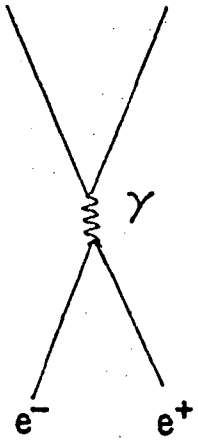

A

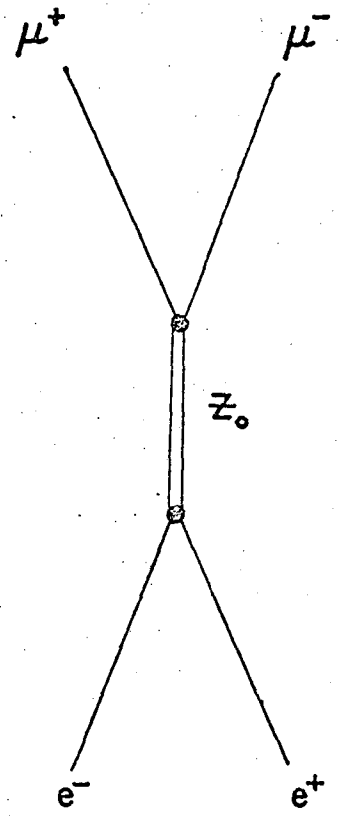

B

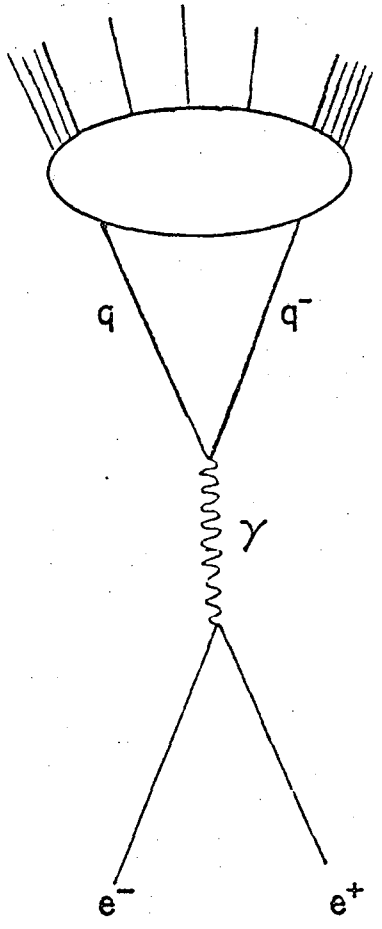

C

Figure 1

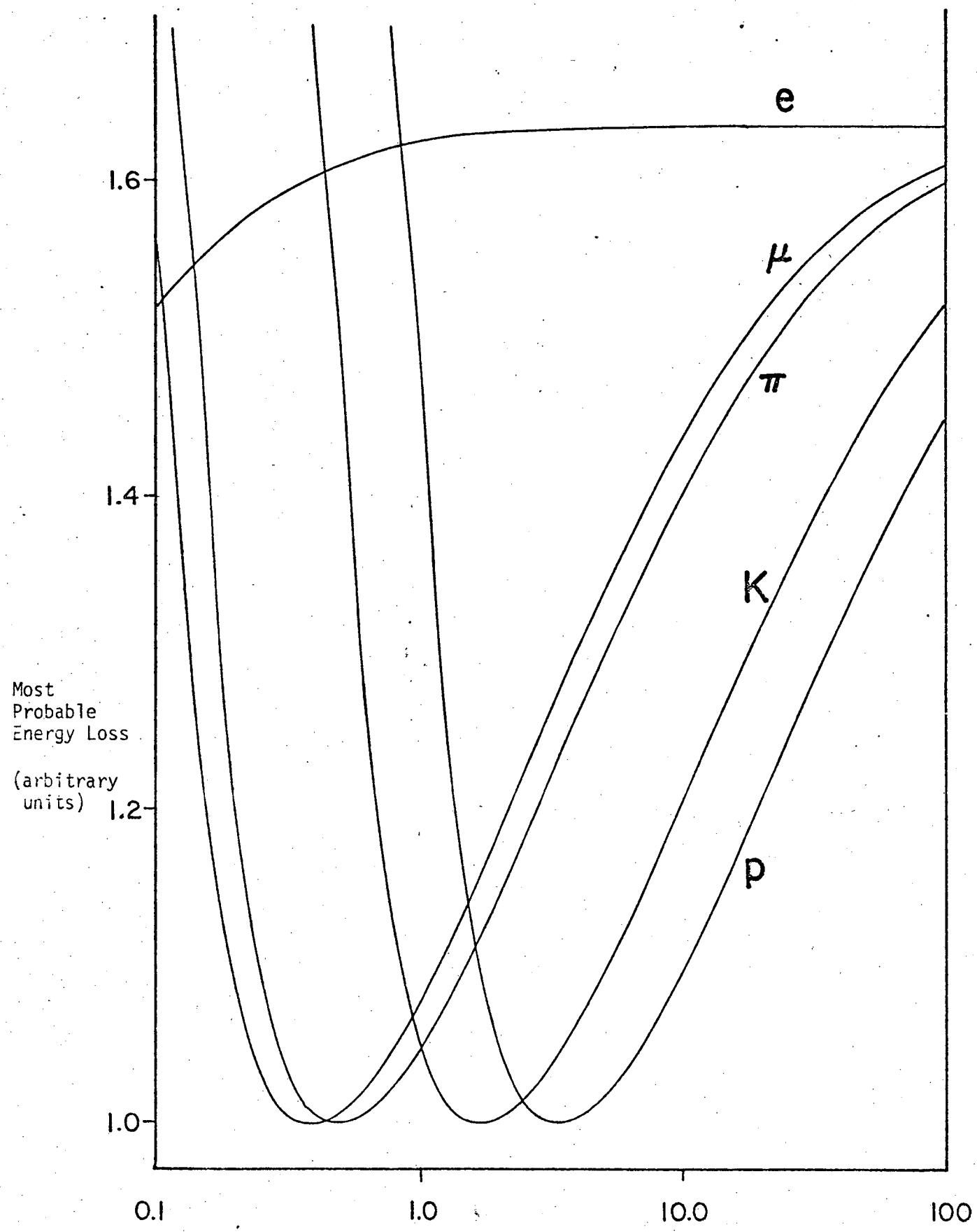
e
μ
π
K
p
1.6
1.4
1.2
1.0
Most
Probable
Energy Loss
(arbitrary
units)
0.1
1.0
10.0
100
PARTICLE MOMENTUM (GeV/c)

Figure 2

MEASURED ENERGY LOSS SPECTRUM OF 800 MeV/c PIONS IN 4mm OF 80 % Ar + 20 % CH_4 (10 ATMOSPHERES)

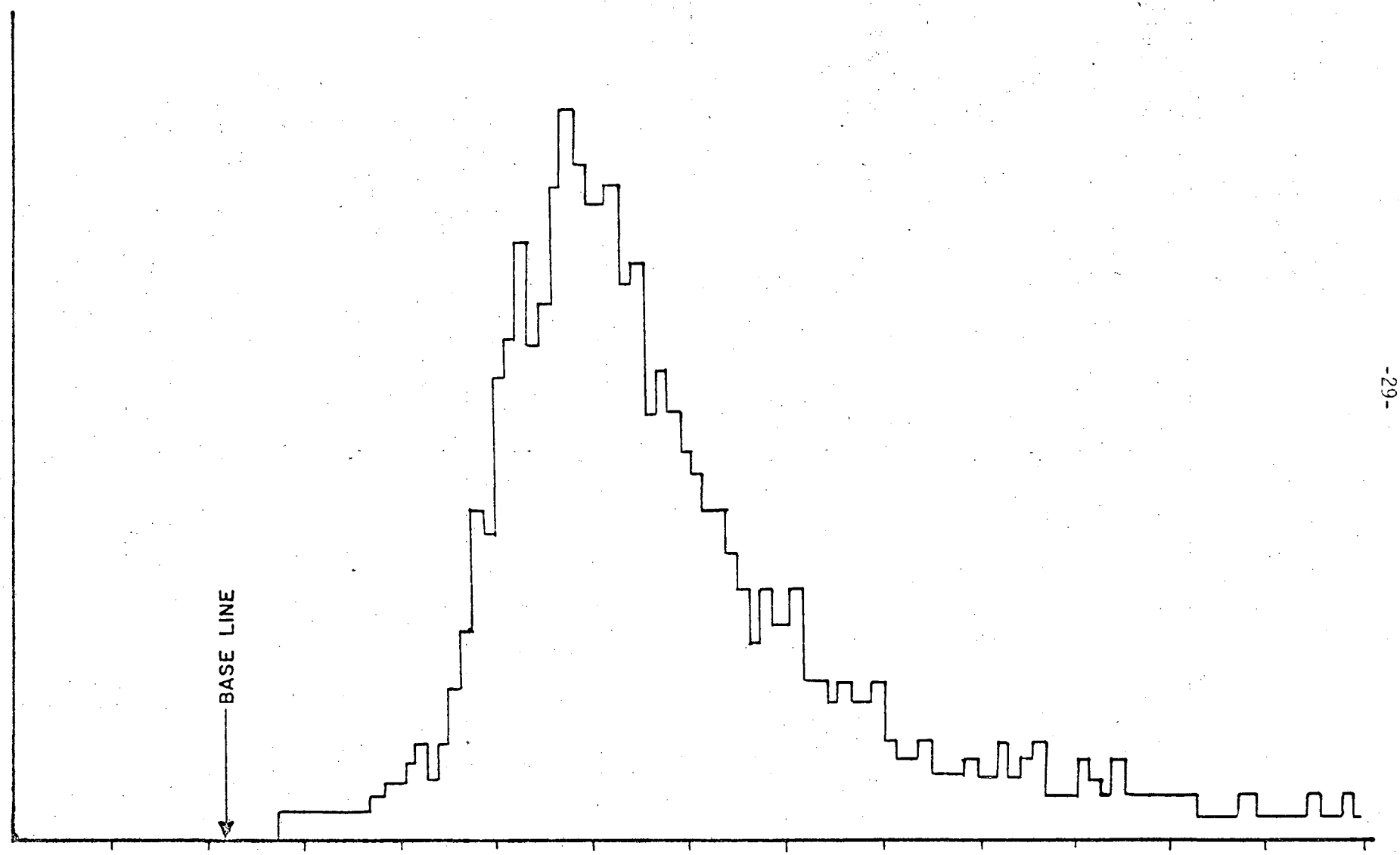

Figure 3

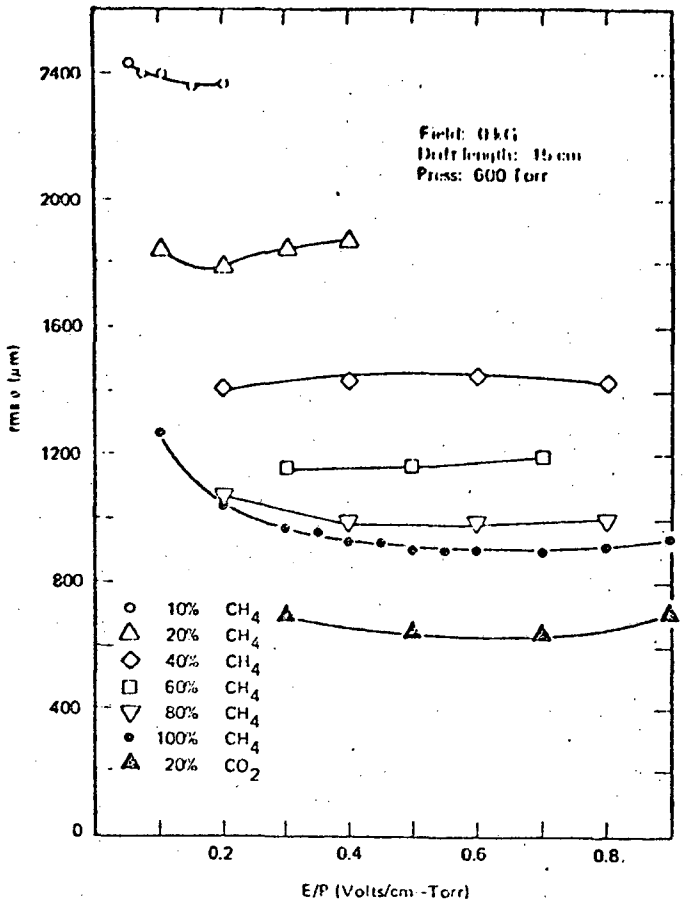
Field: 0 kG
Drift length: 15 cm
Press: 600 Torr
10% CH4
20% CH4
40% CH4
60% CH4
80% CH4
100% CH4
20% CO2
rms σ (μm)
E/P (Volts/cm-Torr)

(a)

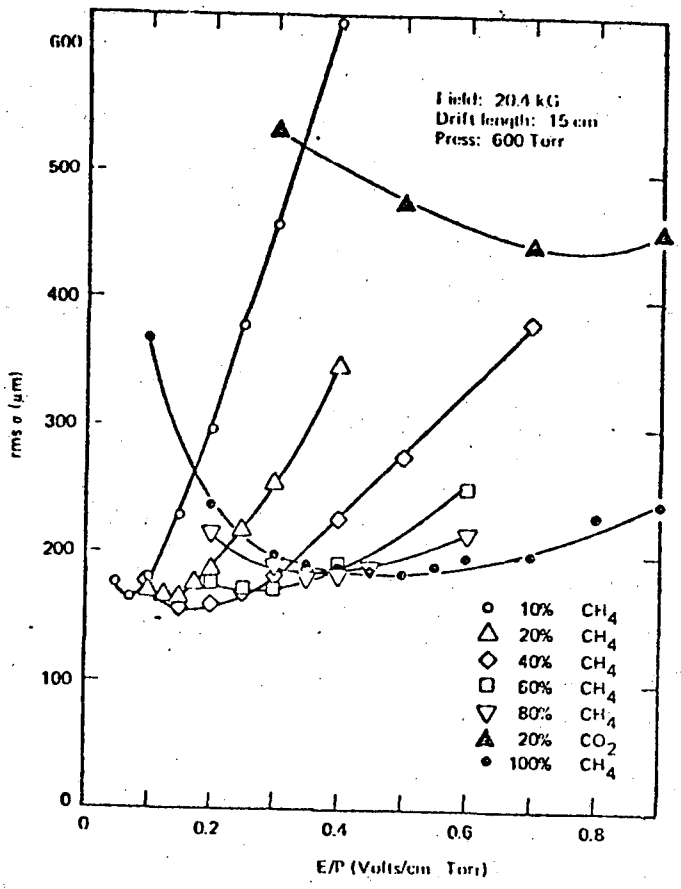
Field: 20.4 kG
Drift length: 15 cm
Press: 600 Torr
10% CH4
20% CH4
40% CH4
60% CH4
80% CH4
20% CO2
100% CH4
rms σ (μm)
E/P (Volts/cm Torr)

(b)

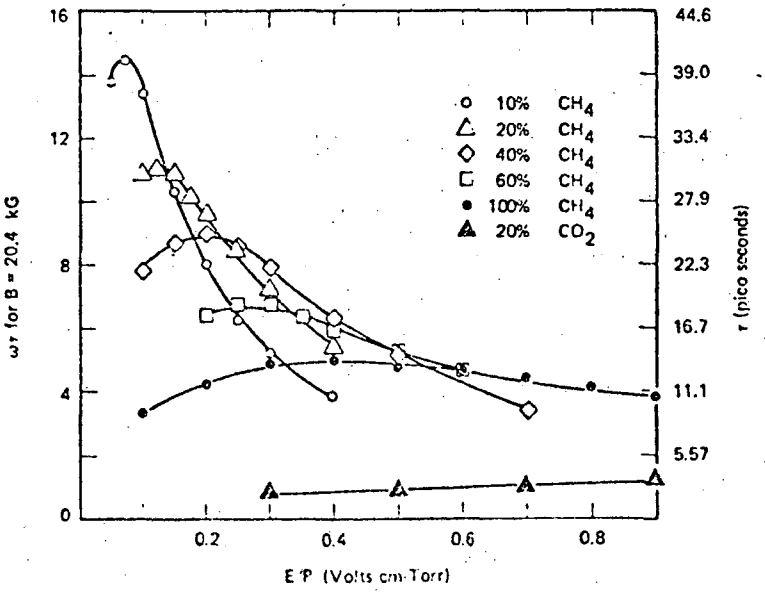
10% CH4
20% CH4
40% CH4
60% CH4
100% CH4
20% CO2
ωτ for B = 20.4 kG
τ (pico seconds)
E/P (Volts cm-Torr)

(c)

Figure 4

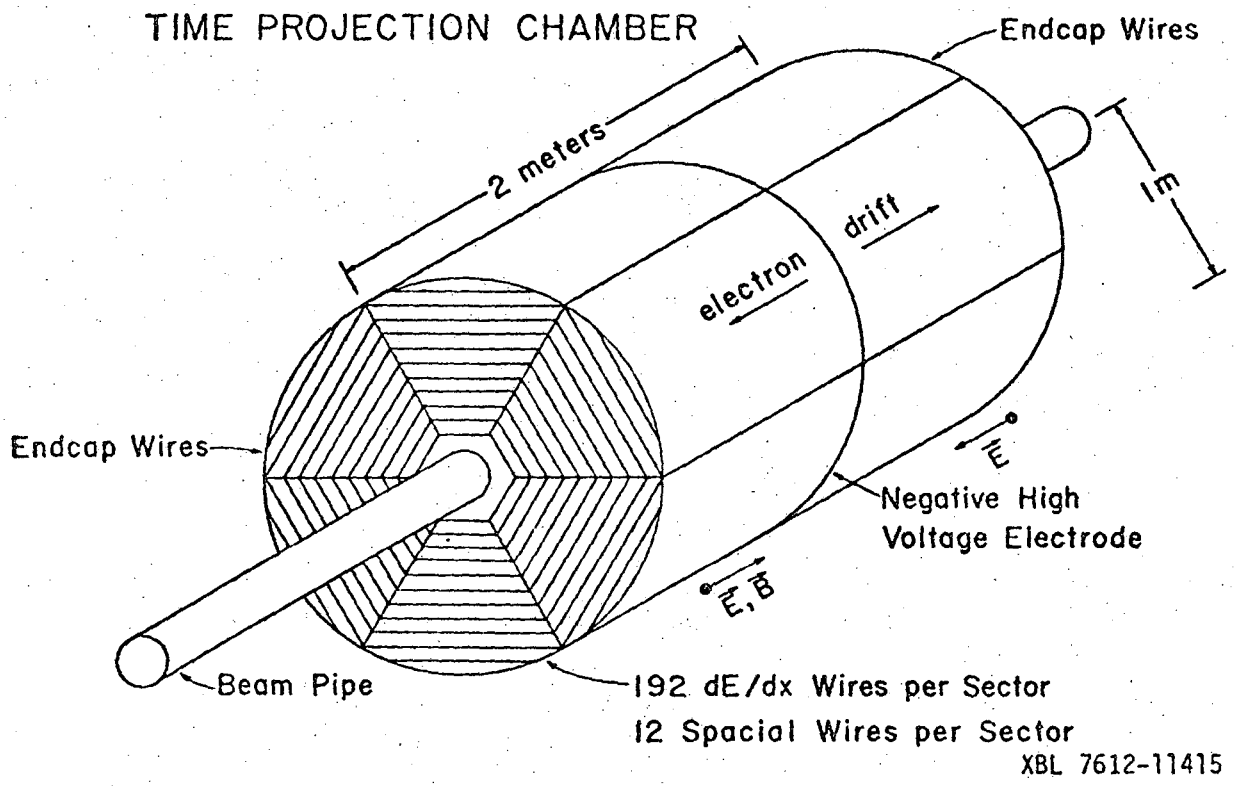
TIME PROJECTION CHAMBER
Endcap Wires
2 meters
1m
drift
electron
Endcap Wires
Negative High
Voltage Electrode
Beam Pipe
192 dE/dx Wires per Sector
12 Spacial Wires per Sector
XBL 7612-11415

Figure 5

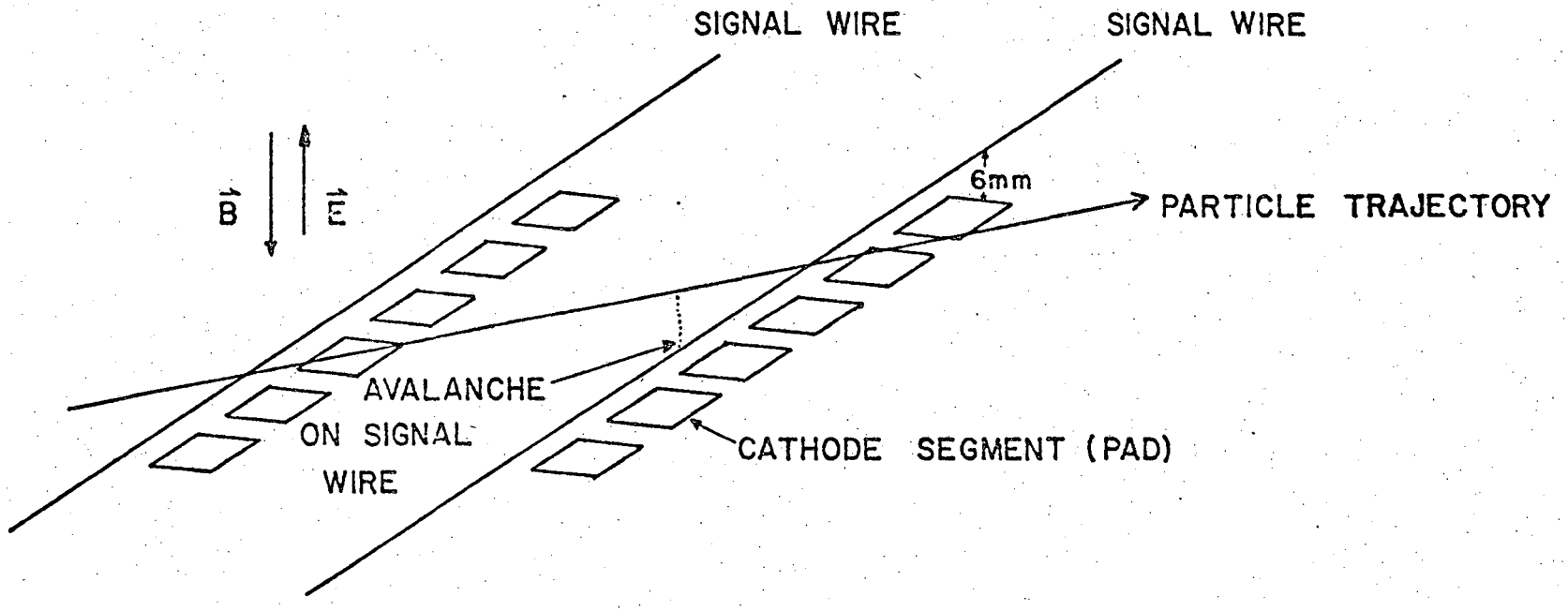
SIGNAL WIRE
SIGNAL WIRE
$\vec{B}$
$\vec{E}$
6mm
PARTICLE TRAJECTORY
AVALANCHE
ON SIGNAL
WIRE
CATHODE SEGMENT (PAD)

Figure 6

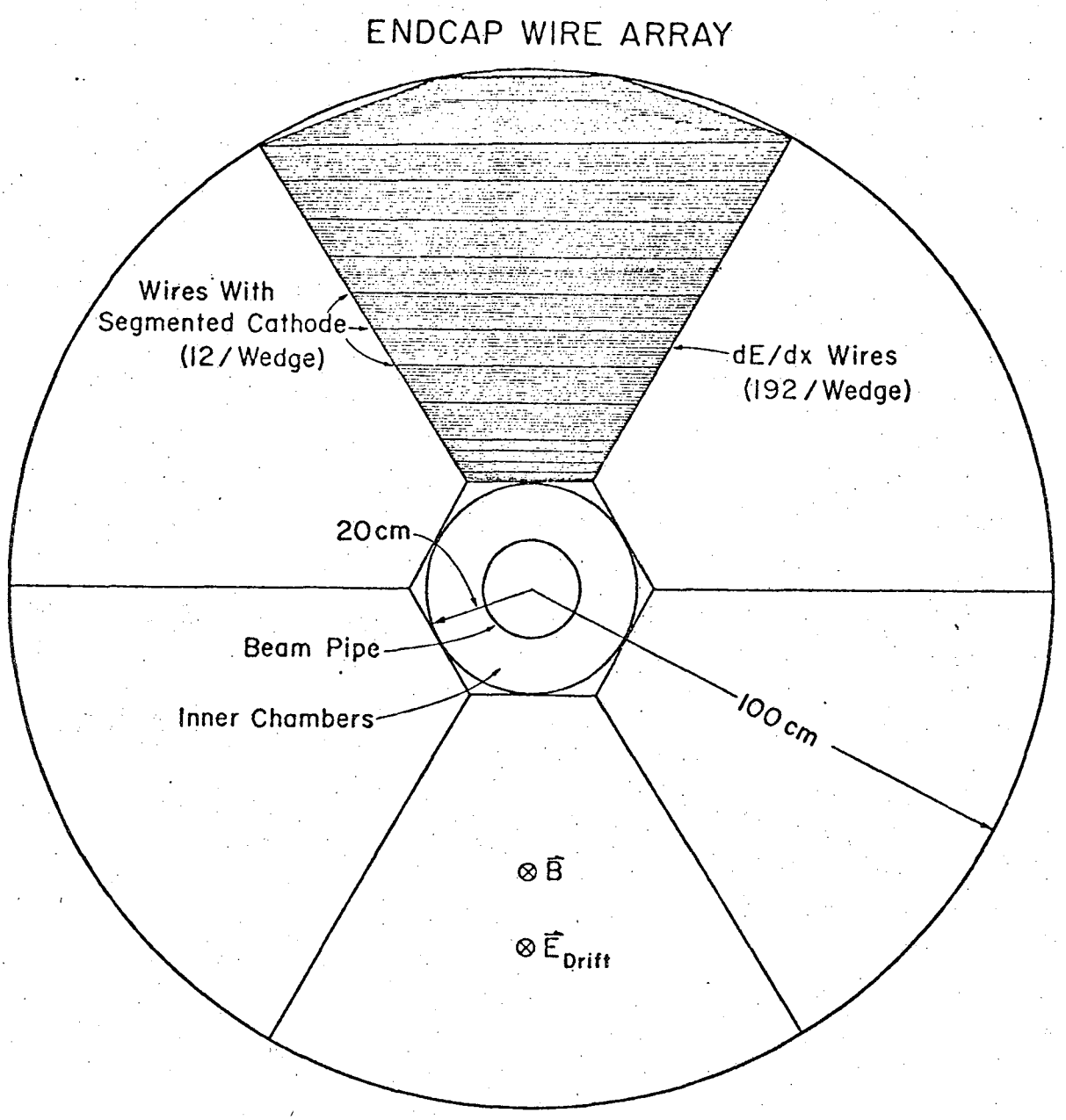
ENDCAP WIRE ARRAY
Wires With
Segmented Cathode
(12 / Wedge)
dE/dx Wires
(192 / Wedge)
20cm
Beam Pipe
Inner Chambers
100cm
⊗ B
⊗ E Drift
XBL 7612-11328

Figure 7

TOWER = -15.0 KV
GROUND E FIELD = .324890E+04

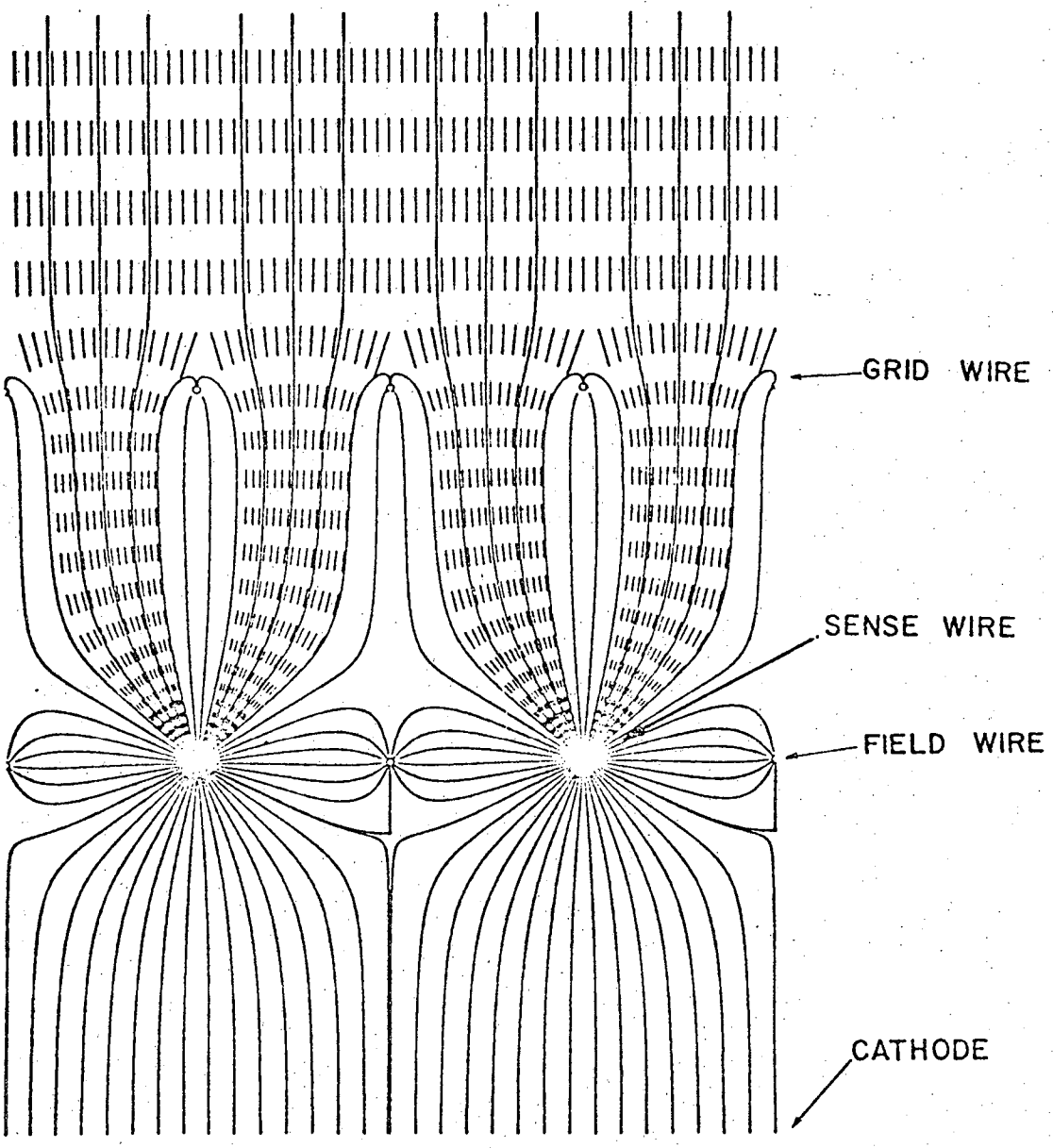

R = .40 MILL 1.50 MILL 1.50 MILL 1.50 MILL
V = 3750.0 400.0 0.0 0.0
E = .558408E+06 .456895E+05 .115137E+05 .113046E+05

XBL 782-7127

Figure 8

TEST PRESSURE VESSEL

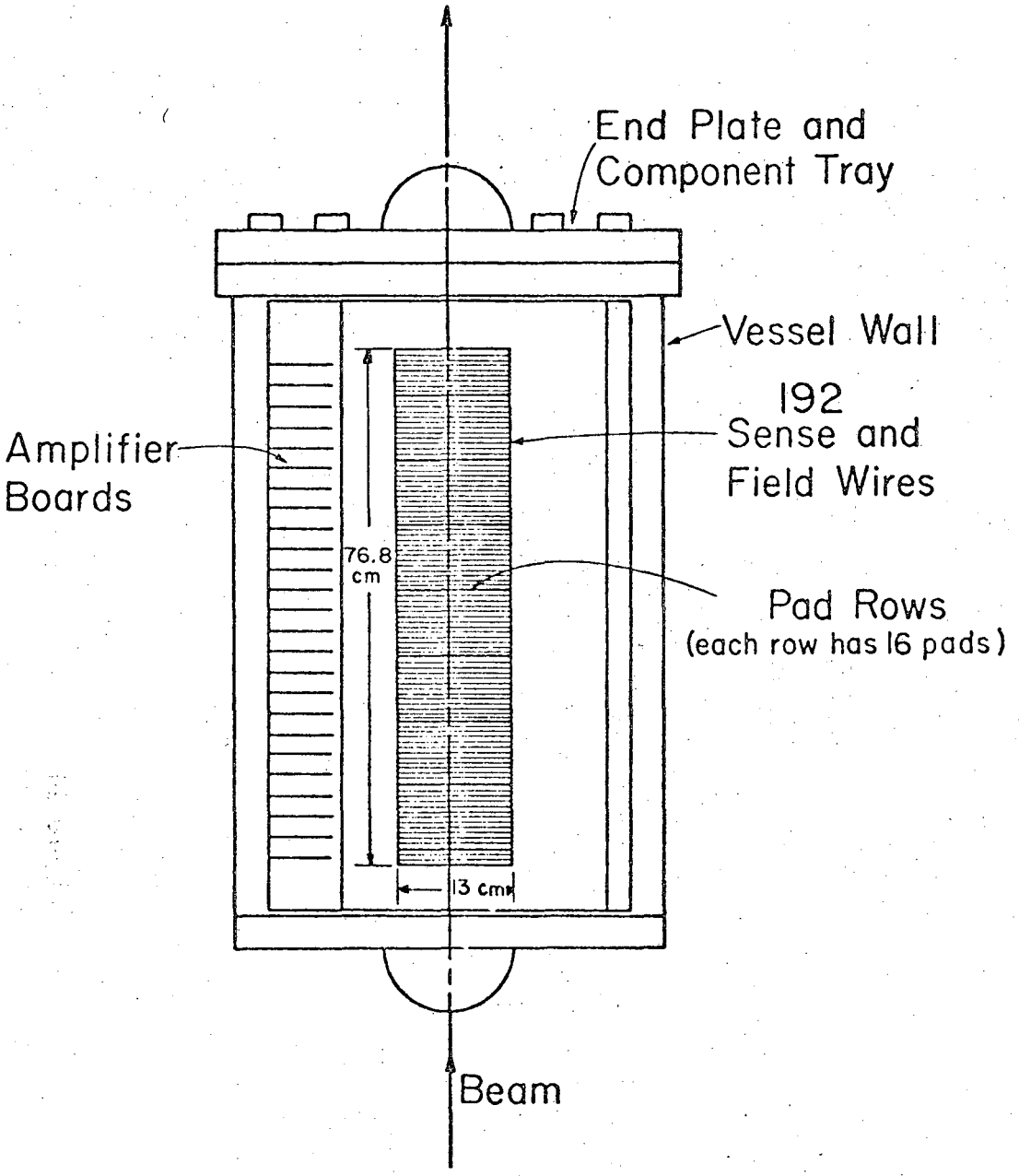

XBL 7612-11261A

Figure 9

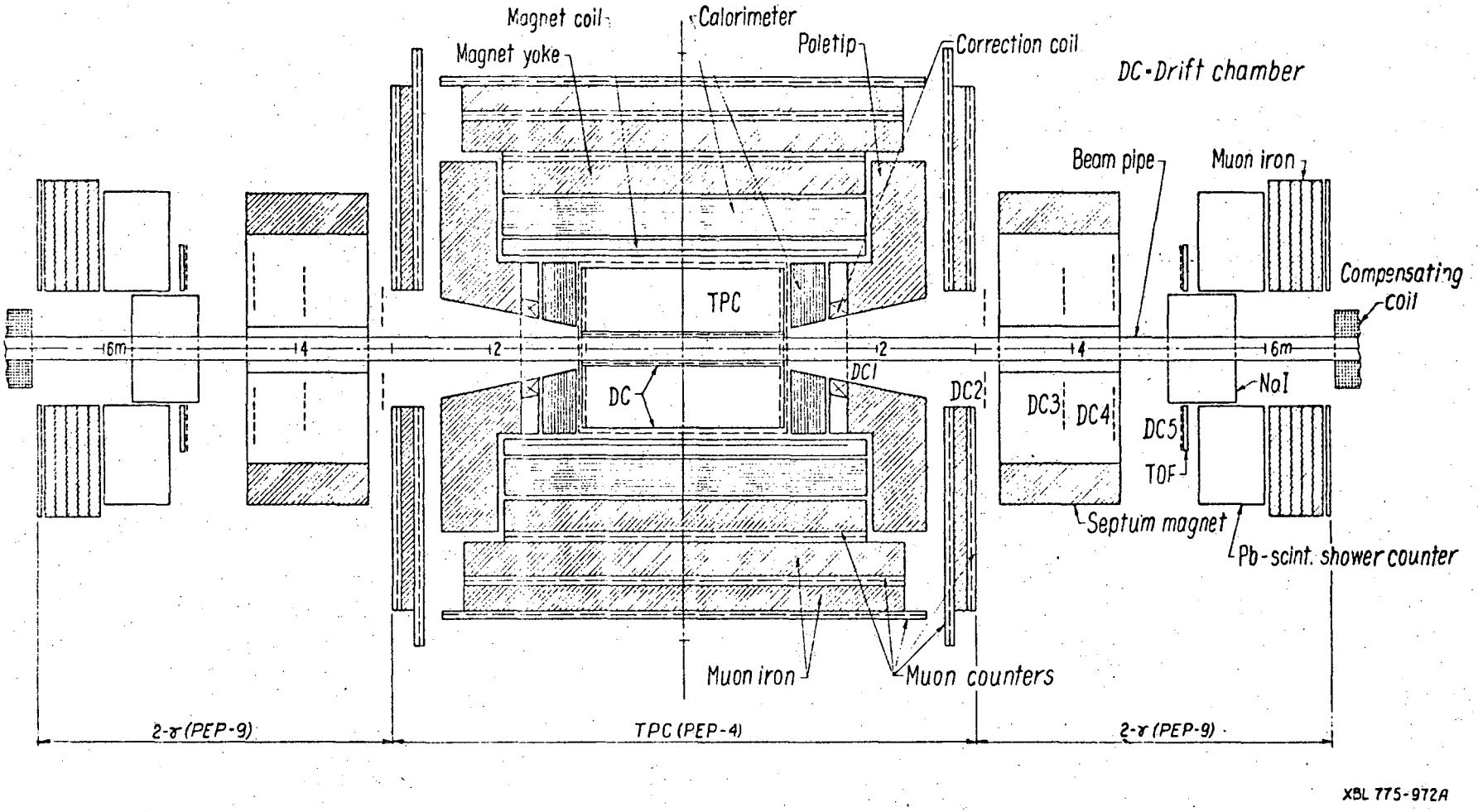
Magnet coil
Calorimeter
Magnet yoke
Poletip
Correction coil
DC - Drift chamber
Beam pipe
Muon iron
Compensating coil
TPC
16m
4
2
2
4
16m
DC1
DC
DC2
DC3
DC4
DC5
TOF
NaI
Septum magnet
Pb-scint. shower counter
Muon iron
Muon counters
2-γ (PEP-9)
TPC (PEP-4)
2-γ (PEP-9)
XBL 775-972A

Figure 10

TOWER = -15.0 KV
GROUND E FIELD = .283660E+04

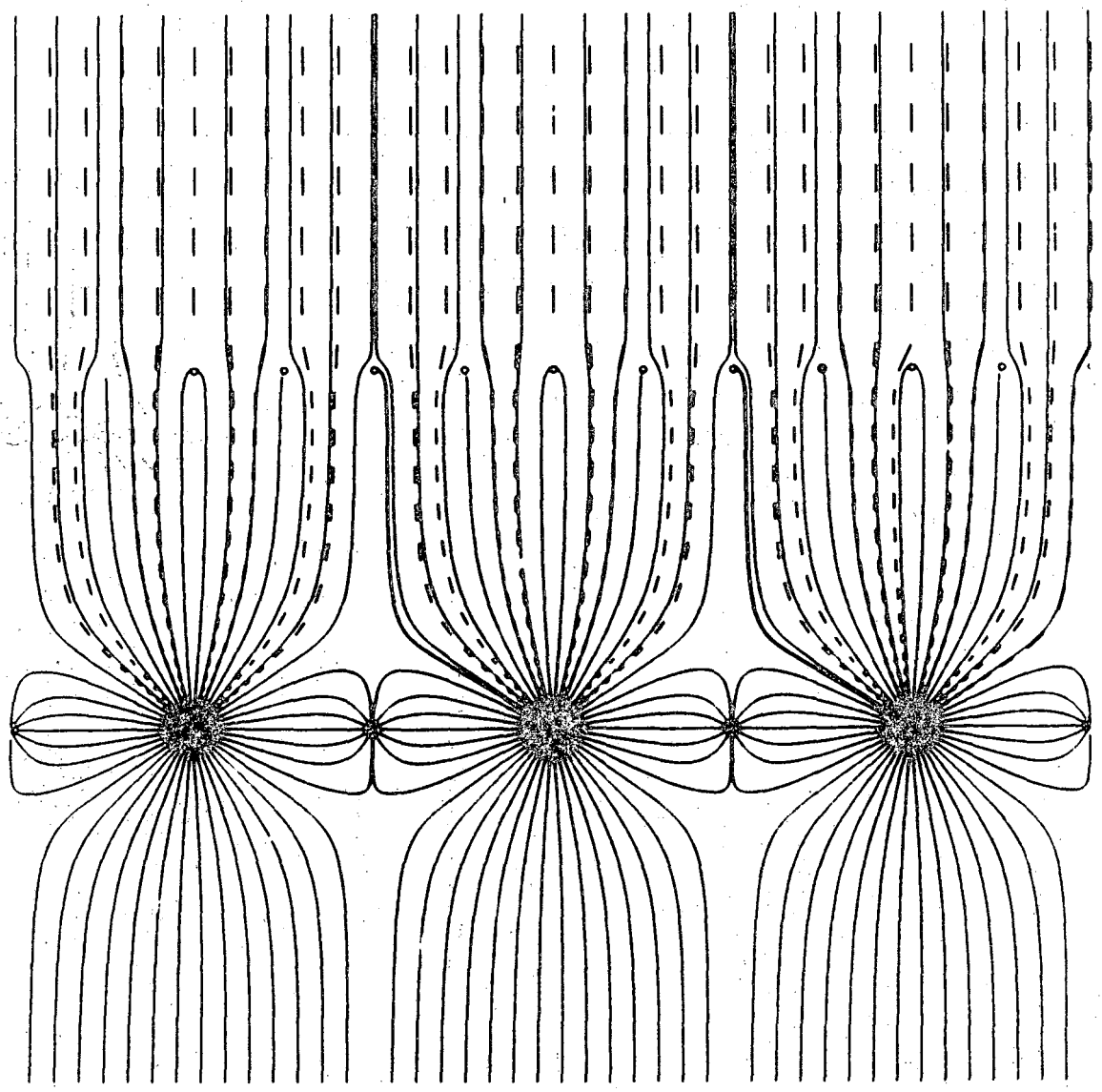

R = .40 MILL 1.50 MILL 1.50 MILL 1.50 MILL
V = 3300.0 350.0 0.0 0.0 0.0
E = .494047E+06 .393847E+05 .516670E+04 .498793E+04 .506437E+04

XBL 7810-11987

Fig. 11a

TOWER = -15.0 KV
GROUND E FIELD = .283660E+04

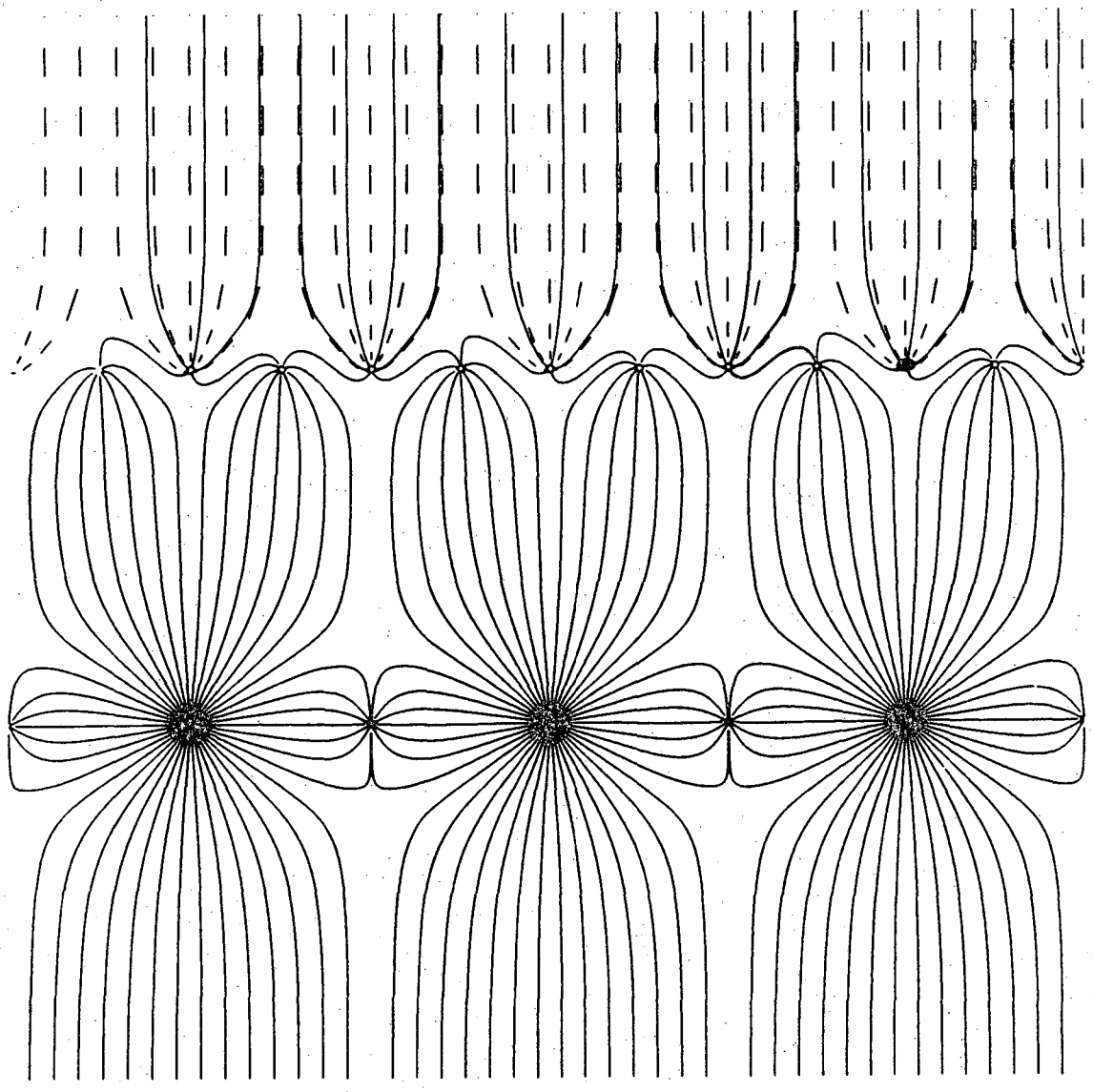

R = .40 MILL 1.50 MILL 1.50 MILL 1.50 MILL
V = 3300.0 350.0 250.0 250.0 -250.0
E = .494047E+06 .393847E+05 .188137E+05 .189880E+05 .280123E+05

XBL 7810-11986

Fig. 11b

This report was done with support from the Department of Energy. Any conclusions or opinions expressed in this report represent solely those of the author(s) and not necessarily those of The Regents of the University of California, the Lawrence Berkeley Laboratory or the Department of Energy.

TECHNICAL INFORMATION DEPARTMENT
LAWRENCE BERKELEY LABORATORY
UNIVERSITY OF CALIFORNIA
BERKELEY, CALIFORNIA 94720